

## Polarization tunability and analysis for observing magnetic effects on BL39XU at SPring-8

H. Maruyama,<sup>a\*</sup> M. Suzuki,<sup>b</sup> N. Kawamura,<sup>c</sup> M. Ito,<sup>d</sup> E. Arakawa,<sup>e</sup> J. Kokubun,<sup>f</sup> K. Hirano,<sup>g</sup> K. Horie,<sup>f</sup> S. Uemura,<sup>a</sup> K. Hagiwara,<sup>f</sup> M. Mizumaki,<sup>b</sup> S. Goto,<sup>b</sup> H. Kitamura,<sup>c</sup> K. Namikawa<sup>e</sup> and T. Ishikawa<sup>c</sup>

<sup>a</sup>Faculty of Science, Okayama University, 3-1-1 Tsushima-Naka, Okayama, Okayama 700-8530, Japan, <sup>b</sup>SPring-8, Japan Synchrotron Radiation Research Institute, 323-3 Mihara, Mikazuki, Sayo, Hyogo 679-5198, Japan, <sup>c</sup>SPring-8, Harima Institute, The Physical and Chemical Institute (RIKEN), 323-3 Mihara, Mikazuki, Sayo, Hyogo 679-5143, Japan, <sup>d</sup>Faculty of Science, Himeji Institute of Technology, 1475-2 Kanaji, Kamigouri, Ako, Hyogo 678-1297, Japan, <sup>e</sup>Tokyo Gakugei University, 4-1-1 Nukui-Kita, Koganei, Tokyo 184-8501, Japan, <sup>f</sup>Faculty of Science and Technology, Science University of Tokyo, 2641 Yamazaki, Noda, Chiba 278-8510, Japan, and <sup>g</sup>Institute of Material Structure Science, KEK, 1-1 Oho, Tsukuba, Ibaraki 305-0801, Japan. E-mail: maruyama@mag.okayama-u.ac.jp

(Received 9 June 1999; accepted 31 August 1999)

Polarization tunability and analysis of X-rays is one of the most advancing features of third-generation synchrotron radiation sources. In order to apply such developments to the observation of magnetic effects, a diffractometer for X-ray magnetic absorption and scattering experiments was constructed on BL39XU at SPring-8. The efficiency of the apparatus is clearly demonstrated by several observations of the magnetic effects. In particular, a diamond phase plate plays an essential role in regulating both circular and linear polarization states.

**Keywords:** third-generation synchrotron radiation; polarization tunability and analysis; diamond phase plates; magnetic effects.

### 1. Introduction

Polarization tunability of incident photons and polarization analysis of scattered X-rays may be promising elements for material science studies at third-generation synchrotron radiation sources. Such advancements can be efficiently performed in low-emittance rings and will induce new techniques for material characterization. In particular, the tunability and analysis of polarized X-rays are a crucial factor for the study of magnetic properties using absorption, diffraction or emission techniques on the basis of linear or circular polarization. For this reason a combination of linear undulator and phase retarder was adopted as a polarized photon source for beamline 39XU at SPring-8 (Maruyama, 1996), and a diffractometer was installed for X-ray magnetic absorption and scattering experiments. In this report we briefly present the main characteristics of the apparatus and demonstrate its feasibility for observing magnetic effects through X-ray resonant magnetic scattering (XRMS), X-ray scattering caused by anisotropy of the tensor of susceptibility (ATS), X-ray magnetic circular dichroism (XMCD) and X-ray magnetic diffraction (XMD). It should be emphasized that the phase retarder using a diamond single crystal plays an essential role for regulation of the polarization states, being indispensable

for measuring the magnetic effects with an improved data quality.

### 2. Apparatus and polarization analysis

Linearly polarized X-rays emitted from a linear undulator are monochromated by a standard rotated-inclined double-crystal monochromator (Ishikawa, 1996). A flat Pt-coated mirror was also installed for higher harmonics rejection. The primary X-ray beam passes into the experimental hutch through a Be window. The apparatus is composed of a phase retarder assembly, a three-circle diffractometer, and another four-circle goniometer for polarization analysis, as schematically shown in Fig. 1. The phase retarder, placed at the most upstream position in the hutch, can function as both a quarter-wave plate, which converts from linear to circular polarization, and a half-wave plate, which generates vertical linear polarization (Ishikawa *et al.*, 1992). A synthetic diamond (111) crystal slab of thickness 0.73 mm was fixed onto the crystal holder of a standard goniometer, with the rotation axis tilted at 45° from the polarization plane of the primary X-ray beam, and was operated around the 220 reflection in transmission (Laue) geometry. The three-circle diffractometer, mounted on a large *x*-*z* translation stage, consists of a 2 $\Theta$ -arm, an  $\Omega$ -

circle to carry the sample with an electromagnet and a cryostat, and an additional  $\omega$ -arm that is available for mounting another detector or optional axes for sample orientation. According to the experimental requirements, any polarization state of the incident X-ray beam irradiating the sample can be optimized using the phase retarder. The four-circle goniometer mounted on the  $2\theta$ -arm functions as a linear polarization analyzer, whereby X-rays scattered by the sample can be separated into horizontal ( $\pi$ ) and vertical ( $\sigma$ ) polarization components. An Si(331) channel-cut crystal, installed in the  $\chi$ -circle together with a scintillation counter, was prepared as the analyzer for a photon energy range around 7 keV, so that the degree of linear or circular polarization can be estimated from the dependence of X-ray intensity on the  $\chi$ -angle.

Using this experimental set-up we first characterized the primary X-ray beam with horizontal linear polarization near the Fe *K*-edge. Secondly, the diamond phase plate was regulated so as to convert linear polarization to circular polarization. Then the degree of polarization was assessed as a function of offset angle  $\Delta\theta_B$  from the Bragg condition. Finally, the offset angle needed to generate the vertical linear polarization was determined and the polarization state was estimated. The angle variation of the X-ray intensity for these three polarization states is summarized in Fig. 2. Under the adjusted offset angle the dependence of the X-ray intensity on the  $\chi$ -angle can be expressed as follows,

$$I(\chi) = S_0 + S_1 \cos 2\chi + S_2 \sin 2\chi, \quad (1)$$

where  $S_0$  is an angle-independent term,  $S_1$  and  $S_2$  correspond to components of the Stokes vector, and  $\chi$  is the azimuthal angle of the four-circle goniometer (see Fig. 1). For linear polarization, the degree of the  $\pi$  and  $\sigma$  polarization ( $P_L$ ) can, in principle, be estimated from the value of the  $S_1/S_0$  ratio. The degree of circular polarization ( $P_C$ ) can also be evaluated as  $[1 - (S_1/S_0)^2 - (S_2/S_0)^2]^{1/2}$ , under the assumption that no unpolarized component is present. Since this beamline is equipped with a linear undulator,

horizontal linear polarization is originally available. As a result of the polarization analysis, the primary X-ray beam monochromated at 7.1195 keV was evaluated to be  $P_L \simeq 0.998$  by a logarithmic fitting to equation (1). This value is in good agreement with that obtained in theoretical *SPECTRA* calculations (Kitamura, 1993), and such a high rate is suitable for conversion to other polarization states by the phase plate. Indeed, when we adjust the offset angle to be equal to the  $\pi/2$  phase shift between the  $\pi$  and  $\sigma$  polarizations, the primary X-ray beam is converted to circularly polarized X-rays. The polarization analysis gave us the value of  $P_C \simeq 0.996$ . Such a high rate can be retained over a broad energy range by regulating the offset angle, which depends on the wavelength, the Bragg angle, the X-ray path length in the crystal *etc.* (Hirano *et al.*, 1992). Moreover, it is also possible to generate the vertical linear polarization: when the offset angle is adjusted to the  $\pi$  phase shift, the primary  $\pi$  polarization state can be rotated to the  $\sigma$  polarization state. In this case the degree of linear polarization was estimated to be  $P_L \simeq 0.82$ . Although this is a high rate, the degree of polarization is not sufficient, which is probably due to less matching of the phase plate thickness for angular divergence of the primary X-ray beam. A further improvement is required for observing optical activities using linear polarization, *e.g.* linear birefringence, linear dichroism *etc.* Vertical linear polarization is suitable for magnetic scattering experiments in the horizontal scattering plane. Results of an efficiency test of the phase retarder assembly have been reported elsewhere (Suzuki, Kawamura, Goto *et al.*, 1998).

### 3. Results and discussion

The phase retarder can easily and efficiently alternate between  $\pi$  and  $\sigma$  polarization. This performance was tested by the following two diffractometry measurements. First, XRMS at the Fe *K*-edge was undertaken for the 200 Bragg reflection of an Fe single crystal that is shaped like a disc of diameter 6 mm and with (100) oriented parallel to the

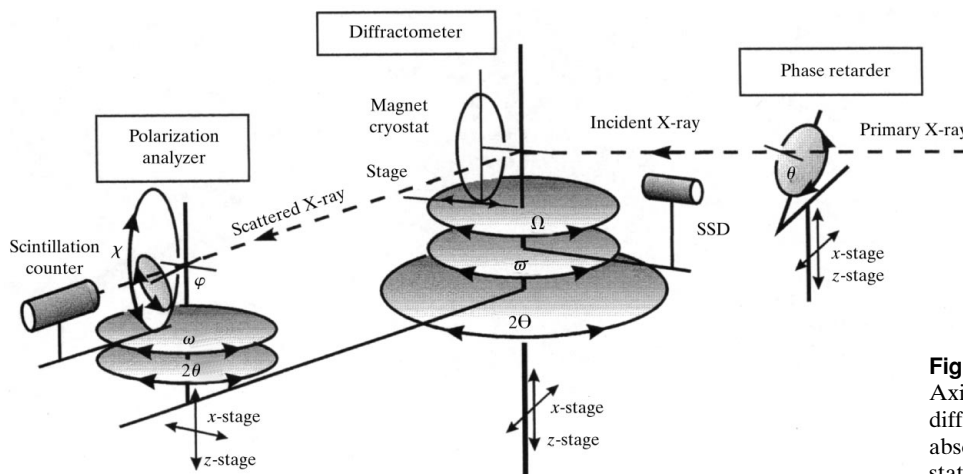


**Figure 1**

Axis configuration of the BL39XU diffractometer for X-ray magnetic absorption and scattering. SSD: solid-state detector.

surface. In particular, we paid attention to observing differences in the dichroic spectra recorded for the  $\pi$  and  $\sigma$  polarization states. The dichroic effect is manifested by the flipping ratio, defined as

$$R_a = (I^\uparrow - I^\downarrow)/(I^\uparrow + I^\downarrow), \quad (2)$$

where  $I^\uparrow$  ( $I^\downarrow$ ) indicates the intensity of scattered X-rays for the magnetization parallel (antiparallel) to the cross products ( $\mathbf{k} \times \mathbf{k}'$ ) of the wave vectors of the incident and scattered X-rays. A magnetic field of 2 kOe (1 kOe = 1000/4 $\pi$  A m<sup>-1</sup>) was applied parallel to the [100] direction and reversed every 2 s. Data were accumulated 20 times at each energy point in the parallel and antiparallel directions. Fig. 3 shows the  $R_a$  spectrum around the Fe *K*-edge using the horizontal or vertical linearly polarized X-ray beam. The spectrum, usually recorded with horizontal polarization, shows a dispersion-like profile near the edge, which is in good agreement with the early data taken at a second-generation synchrotron radiation facility (Namikawa, 1997). On the other hand, the spectrum recorded under vertical polarization indicates no change of sign at the higher-energy side. This difference could be discussed in terms of the polarization dependence of the dichroic term in resonant magnetic scattering (Hannon *et al.*, 1988), and may provide detailed information both on the spin and orbital contributions and on the electric dipole and quadrupole transitions.

Another demonstrative phenomenon for the change of the polarization state is the ATS scattering, which can be observed as a forbidden reflection near the absorption edge

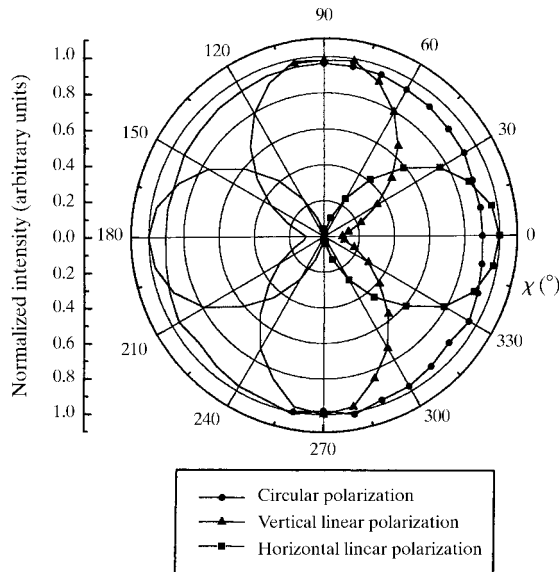


**Figure 2**

X-ray intensity as a function of the azimuthal  $\chi$ -angle for the circular and linear (horizontal and vertical) polarization states. The variations are displayed by polar coordinates. Measurements were made in the range  $-105^\circ$  to  $+105^\circ$ , and the solid line in the portion from  $90^\circ$  to  $270^\circ$  was symmetrically illustrated using the data.

due to a breakdown of the extinction rule. For this experiment a single crystal of FeS<sub>2</sub> (pyrite) was prepared. The angle variation  $I(\chi)$  of the (001) forbidden reflection was measured around the Fe *K*-edge using the polarization analyzer assembly. As a result, a convertible change between the  $\pi$  and  $\sigma$  polarizations was definitely confirmed by the polarization analysis, *i.e.* when the polarization of the incident X-ray beam was the pure  $\pi$ -state, the polarization of the scattered X-ray beam was completely alternated to the  $\sigma$  polarization, and *vice versa* (Nagano *et al.*, 1996). The  $\sigma$  polarization, generated from the phase retarder operated as a half-wave plate, will be widely available.

Circularly polarized X-rays are also indispensable for measuring magneto-optical effects. The phase plate is capable of producing circularly polarized X-rays and has been applied to XMCD measurements (Giles *et al.*, 1994; Hirano & Maruyama, 1997). In the present case of the Fe *K*-edge, when the offset angle was adjusted to  $\sim 103$  arcsec a value of  $P_C > 0.99$  was obtained. Moreover, the helicity can be easily alternated between the  $\pm 103$  arcsec offset angle, which means there is a possibility of helicity alternation. This advantage has been actually developed into the so-called helicity-modulation method that has led to a marked improvement in accuracy in a dichroic spectrum (Suzuki, Kawamura, Mizumaki *et al.*, 1998). Fig. 4 shows the Fe *K*-edge XMCD in pure Fe. The spectrum was recorded in conventional transmission mode with fixed positive helicity and reversing applied magnetic field. The magnetic field of 1 kOe was tilted  $60^\circ$  away from the incident X-ray beam and applied parallel to the plane of a 5  $\mu\text{m}$ -thick Fe foil. Data were accumulated ten times at each energy point while the field direction was reversed at

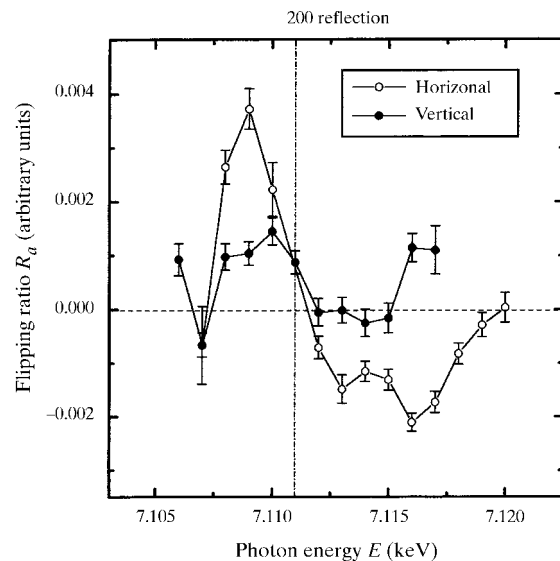


**Figure 3**

Flipping ratio of XRMS for the 200 Bragg reflection around the Fe *K*-edge under horizontal and vertical polarization. The error bars display the standard deviation. The vertical dot-dash line shows the absorption-edge energy.

intervals of 2 s. This spectrum clearly shows a larger dichroic signal, a better statistical accuracy and a better efficiency in comparison with the spectrum recorded under identical conditions at a second-generation synchrotron radiation facility (Maruyama *et al.*, 1991). These benefits may result from the high-flux beam and the high degree of circular polarization. When the sign of the offset angle was changed, the XMCD spectrum was completely reversed.

Finally, elliptically polarized X-rays are essential for measuring spin and orbital moment densities using the XMD technique (Lovesey & Collins, 1996). The polarization state with both linear and circular components can be controlled by tuning the offset angle of the phase plate, so

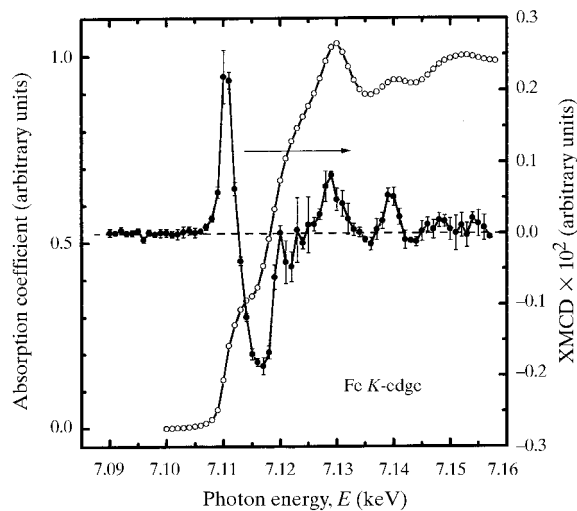


**Figure 4**

Fe *K*-edge XMCD spectrum in pure Fe foil. The error bars display the standard deviation. The XANES spectrum normalized in the conventional way is also denoted by open circles. The XMCD spectrum was subjected to normalization and correction with respect to the field direction.

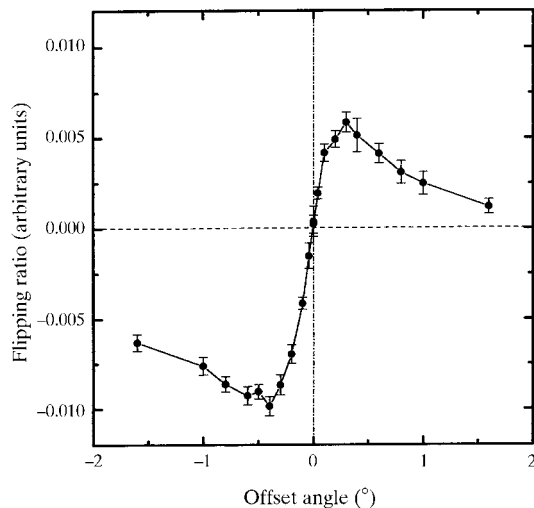


**Figure 5**

Variation of flipping ratio in XMD with offset angle of the phase plate, which was recorded in the  $90^\circ$  scattering configuration. The vertical dot-dash line corresponds to the Bragg condition.

that the monochromatic X-ray method was applied to the XMD measurement for an Fe single crystal, in which the Bragg diffraction from a (220) plane was recorded by tuning both photon energy and polarization state. When we adjusted the photon energy to  $E = 8.65$  keV ( $\lambda = 1.433$  Å), the configuration of  $90^\circ$  scattering could be maintained. The magnetic effect is also manifested by the flipping ratio described by equation (2). In this test we measured the variation of  $R_a$  with the offset angle, as shown in Fig. 5. The ratio reached an amplitude of 1%, which was about twice as large as that measured at the second-generation synchrotron radiation facility (Ito & Hirano, 1997). Since the value of  $R_a$  is proportional to the polarization factor  $P_C/(1 - P_L)$ , this figure shows the tunability of elliptical polarization. It is clearly observed, however, that the variation is asymmetrical. It turned out that the polarization vector slightly rotated around the wavevector of the transmitted X-ray beam and the polarization states depended on the operation mode of the synchrotron radiation source (Ito, 1999). It should be noted that the tunability of the polarization factor is advantageous to the enhancement of the magnetic effect.

#### 4. Conclusions

The performance of the polarization tunability and analysis at the SPring-8 photon source has been demonstrated by several magnetic effects. The efficiency of the apparatus for X-ray magnetic absorption and scattering has also been shown. The diamond phase plate and the channel-cut analyzer functioned effectively. It should be noted that the phase retarder plays an essential role in regulating both the circularly and linearly polarized X-rays. The polarization analysis of scattered X-rays may provide us with detailed information on the electronic structure and also extend XRMS into antiferromagnetic materials. X-ray beams with a high flux and a high-rate polarization are suitable for not only observation of magnetic effects with high statistical accuracy but also for experiments under extreme conditions.

The authors express their thanks to Professor H. Yamazaki, Professor N. Sakai, Professor K. Ishida, Dr T. Iwazumi, Mr M. Sato, Dr A. Koizumi and Dr S. Hayakawa for their cooperation and support, and also thank Dr J. Chaboy-Nalda for critical reading of the manuscript. This work was carried out under the approval of SPring-8 committee Nos. 1997B0153 and 1997B0154.

#### References

- Giles, C., Malgrange, C., Goulon, J., de Bergevin, F., Vettier, C., Dartyge, E., Fontaine, A., Giorgetti, C. & Pizzini, S. (1994). *J. Appl. Cryst.* **27**, 232–240.
- Hannon, J. P., Trammell, G. T., Blume, M. & Gibbs, D. (1988). *Phys. Rev. Lett.* **61**, 1245–1248.

- Hirano, K., Kanzaki, K., Mikami, M., Miura, M., Tamasaku, K., Ishikawa, T. & Kikuta, S. (1992). *J. Appl. Cryst.* **25**, 531–535.
- Hirano, K. & Maruyama, H. (1997). *Jpn. J. Appl. Phys.* **36**, L1272–L1274.
- Ishikawa, T. (1996). *SPring-8 Annual Report 1995*, pp. 38–43. SPring-8, Hyogo 679-5198, Japan.
- Ishikawa, T., Hirano, K., Kanzaki, K. & Kikuta, S. (1992). *Rev. Sci. Instrum.* **63**, 1098–1103.
- Ito, M. (1999). Personal communication.
- Ito, M. & Hirano, K. (1997). *J. Phys. Condensed Matter*, **9**, L613–L617.
- Kitamura, H. (1993). *SPECTRA. Synchrotron Radiation Calculation Program. Version 2.0*. SPring-8, Harima Institute, Hyogo 679-5148, Japan.
- Lovesey, S. W. & Collins, S. P. (1996). *X-ray Scattering and Absorption by Magnetic Materials*. Oxford: Clarendon Press.
- Maruyama, H. (1996). *SPring-8 Annual Report 1995*, pp. 52–54. SPring-8, Hyogo 679-5198, Japan.
- Maruyama, H., Iwazumi, T., Kawata, H., Koizumi, A., Fujita, M., Sakurai, H., Itoh, F., Namikawa, K., Yamazaki, H. & Ando, M. (1991). *J. Phys. Soc. Jpn.* **60**, 1456–1459.
- Nagano, T., Kokubun, J., Yazawa, I., Kurasawa, T., Kuribayashi, M., Tsuji, E., Ishida, K., Sasaki, S., Mori, T., Kishimoto, S. & Murakami, Y. (1996). *J. Phys. Soc. Jpn.* **65**, 3060–3067.
- Namikawa, K. (1997). Unpublished.
- Suzuki, M., Kawamura, N., Goto, S., Mizumaki, M., Kuribayashi, M., Kokubun, J., Horie, K., Hagiwara, K., Ishida, K., Maruyama, H. & Ishikawa, T. (1998). *SPring-8 Annual Report 1997*, pp. 235–237. SPring-8, Hyogo 679-5198, Japan.
- Suzuki, M., Kawamura, N., Mizumaki, M., Urata, A., Maruyama, H., Goto, S. & Ishikawa, T. (1998). *Jpn. J. Appl. Phys.* **37**, L1488–L1490.